

Article

cla-miR164-NO APICAL MERISTEM (CINAM) regulates the inflorescence architecture development of *Chrysanthemum lavandulifolium*

Junzhuo Li^{1,†}, Xiaohui Wen^{1,2,†}, Qiling Zhang¹, Yuankai Tian¹, Ya Pu¹, Jiaying Wang¹, Bo Liu¹, Yihan Du¹ and Silan Dai^{1,*}

¹Beijing Key Laboratory of Ornamental Plants Germplasm Innovation & Molecular Breeding, National Engineering Research Center for Floriculture, Beijing Laboratory of Urban and Rural Ecological Environment, Key Laboratory of Genetics and Breeding in Forest Trees and Ornamental Plants of Ministry of Education, Beijing Forestry University, School of Landscape Architecture, Beijing Forestry University, 35 East Qinghua Road, Beijing, 100083, China

²Flower Research and Development Center, Zhejiang Academy of Agricultural Sciences, Hangzhou 311202, China

*Corresponding author: E-mail: silandai@sina.com

[†]These authors contributed equally to this work.

Abstract

Chrysanthemum × morifolium has great ornamental and economic value on account of its exquisite capitulum. However, previous studies have mainly focused on the corolla morphology of the capitulum. Such an approach cannot explain the variable inflorescence architecture of the chrysanthemum. Previous research from our group has shown that NO APICAL MERISTEM (CINAM) is likely to function as a hub gene in capitulum architecture in the early development stage. In the present study, CINAM was used to investigate the function of these boundary genes in the capitulum architecture of *Chrysanthemum lavandulifolium*, a closely related species of *C. × morifolium* in the genus. Modification of CINAM in *C. lavandulifolium* resulted in an advanced initiation of the floral primordium at the capitulum. As a result, the receptacle morphology was altered and the number of florets decreased. The ray floret corolla was shortened, but the disc floret was elongated. The number of capitula increased significantly, arranged in more densely compounded corymbose synflorescences. The yeast and luciferase reporter system revealed that CLAP1, CLRC2, and CLBD18 target and activate CINAM. Subsequently, CINAM targets and activates CLCUC2a/c, which regulates the initiation of floral and inflorescence in *C. lavandulifolium*. CINAM was also targeted and cleaved by cla-miR164 in this process. In conclusion, this study established a boundary gene regulatory network with cla-miR164-CINAM as the hub. This network not only influences the architecture of capitulum, but also affects compound corymbose synflorescences of the *C. lavandulifolium*. These results provide new insights into the mechanisms regulating inflorescence architecture in chrysanthemum.

Introduction

Chrysanthemum × morifolium is famous for the variable and elegant shape of its capitulum. Its capitulum is formed by ray and disc florets, arranged according to the laws of the Fibonacci series on the receptacle. The morphology, number, direction, relative size, and stability of these two types of florets together determine the capitulum architecture. In addition, a few or more capitula constitute compound corymbose synflorescences at the top of stem and branch of some chrysanthemum varieties and wild species of *Chrysanthemum*. However, the mechanism of inflorescence architectures is obscured by the chrysanthemum's complex genetic background. The study of the mechanism of inflorescence architectures in chrysanthemums is not only beneficial for the targeted breeding of inflorescence architecture in *C. × morifolium*, but also provide a reference point for related research on inflorescence architectures.

Previous studies have shown that the ABC(D)E-class genes in the MADS-box gene family and the CYCLOIDEA 2 (CYC2-like) genes in the TCP gene family play an important role in the corolla formation stage of the capitulum (S8–S10). ABC(D)E-class genes

are mainly involved in determining four whorls of floral organ identity decisions. Silencing of the B-class gene PISTILLATA (PI), APETALA 3 (AP3), or the C-class gene AGAMOUS (AG) was found to result in loss of petal identity on the capitulum [1–3]. The CYC2-like gene is an important floral symmetry gene that affects the morphology of the capitulum by regulating the length and symmetry of the corolla of florets [4–9].

Studies for *Chrysanthemum lavandulifolium* and *Chrysanthemum vestitum* have shown that the floral primordium initiation stage (S5–S7) determines the number, identity, and position of florets on the capitulum, which directly affects capitulum architectures [10, 11]. Our previous research showed that boundary genes such as NO APICAL MERISTEM (NAM), Lateral Organ Boundaries Domain 18 (LBD18), and CUP-SHAPED COTYLEDON 2 (CUC2) are expressed during radial capitulum development and may be key genes for radiating capitulum architectures [12]. In Arabidopsis, NAM/CUCs and LBD18 were found to have functions in establishing organ boundaries and are classified as boundary genes. Boundary genes are expressed at the organ initiation stage of plants to maintain normal organ morphology and function [13, 14].

Received: 7 October 2023; Accepted: 28 January 2024; Published: 22 February 2024; Corrected and Typeset: 1 April 2024

© The Author(s) 2024. Published by Oxford University Press on behalf of Nanjing Agricultural University. This is an Open Access article distributed under the terms of the Creative Commons Attribution License (<https://creativecommons.org/licenses/by/4.0/>), which permits unrestricted reuse, distribution, and reproduction in any medium, provided the original work is properly cited.

The boundary genes have very strict expression domains. Ectopic expression leads to the formation of severe morphological variation in plants [15]. The NAM gene of *Petunia* is required for pattern formation in embryos and flowers [13]. When NAM/CUC was suppressed in *Fragaria* × *ananassa*, *Medicago truncatula*, and *Vigna radiata*, fusion between leaves or petals, a shift from compound leaves to simple leaves, and the phenotype of choripetalous flower to synpetalous flower was shown, suggesting that NAM/CUC plays an important role in maintaining the normal morphology of organs such as flowers and leaves [14, 16–21]. The mechanism of NAM/CUC has been shown to involve direct transcriptional regulation or protein interactions with ABC(D)E class genes and TCP genes [16, 22]. In addition, some members of the NAC gene family are targeted and cleaved by miRNA164. This mechanism is involved in organ initiation and morphological maintenance in several species [14, 18–21, 23, 24]. Many studies have suggested that the miRNA164-NAM/CUC module is essential for the maintenance of normal inflorescence morphology in plants and forms a regulatory network with floral development genes, such as ABC(D)E class genes and TCP genes, to regulate flower morphology. However, the function of the miRNA164-NAM/CUC module in complex inflorescence structures such as the capitulum has not been reported.

Although boundary genes may play an important role in the floral primordium initiation stage of capitulum development, boundary genes' function has been poorly studied in Asteraceae plants. In this study, the biological characteristics of NAM-like (CINAM) in *C. lavandulifolium*, which is a wild species in the genus closely related to *C. × morifolium*, were identified. Furthermore, the CINAM overexpressing transgenic lines were constructed through the stable genetic transformation of *C. lavandulifolium*, we discovered highly specific phenotypes in those transgenic lines. Overexpression of CINAM not only affected the architectures of primary inflorescence, but also secondary inflorescence (a combination of multiple primary inflorescence) of the *C. lavandulifolium*. In the capitulum (primary inflorescence), the receptacle morphology was altered and the number of florets decreased. In addition, the corolla of the ray floret was shortened, but the disc floret was elongated. In the compound corymbose synflorescences (secondary inflorescence), the number of capitulum increased significantly. This result indicates that CINAM affects the inflorescence architectures of *C. lavandulifolium* by regulating the initiation of floral and inflorescence primordia. To analyse the mechanism of action of CINAM, we examined the up- and down-stream genes of CINAM using the yeast reporter system and the luciferase reporter system. The results showed that CINAM responds to the transcriptional activation of the A-class gene *APETALA 1* (*CIAP1*), the E-class genes *C. lavandulifolium* *REGULATOR OF CAPITULUM DEVELOPMENT 2* (*ClRCD2*) and the boundary gene *ClLBD18*, and is also targeted and cleaved by *cla*-miR164. Subsequently, CINAM directly activates downstream boundary genes *ClCUC2a/c* expression, controlling the floral and inflorescence primordia initiation. Our results suggest a boundary gene regulatory network with *cla*-miR164-CINAM as the hub and provide new insights into regulation of chrysanthemum inflorescence architecture.

Results

The biological characteristics of CINAM

Phylogenetic analysis revealed that CINAM (Cl43444) is a member of the NAM clade in the NAC gene family (Fig. S1A, see online supplementary material). One ortholog of CINAM was present in diploid species of *Chrysanthemum* (*Chrysanthemum*

seticuspe, *Chrysanthemum nankingense*, and *Chrysanthemum makinoi*), while three copies were conserved in the hexaploid species *C. × morifolium* (Fig. 1A). Multiple sequence alignment revealed that the sequences of NAM were conserved among *Chrysanthemum* species and all retained the *cla*-miR164 target binding site (Fig. 1B; Fig. S1B, see online supplementary material). The subcellular localization results showed that the CINAM-GFP fusion protein had distinct green fluorescence only in the nucleus, indicating that the CINAM protein was localized in the nucleus with a typical t character of transcription factors (Fig. 1C).

To understand the role of CINAM in the architectures of *C. lavandulifolium* capitulum, the spatiotemporal expression characteristics of CINAM during capitulum development were observed by *in situ* hybridization (Fig. 1D–G). The results showed that CINAM was widely expressed in the inflorescence meristem at the doming stage (S1, Fig. 1D). At the early stage of floret primordia initiation, CINAM was significantly expressed in disc floret primordia (S6, Fig. 1E). At the early stage of corolla primordia formation, the CINAM expression was very strong between floret primordia, especially between disc floret primordia (S8, Fig. 1F). At the late stage of corolla primordia formation, the CINAM expression gradually became weaker between florets (S10, Fig. 1G).

These results tentatively suggest that CINAM has an expression pattern consistent with the boundary genes. It may be involved as a transcription factor in the initiation of floret primordia, especially of the disc floret, from the inflorescence meristem on the *C. lavandulifolium* capitulum. Because the sequence and copy number of NAM is highly conserved among *Chrysanthemum* species, this function of regulating inflorescence differentiation may also be conserved in chrysanthemums.

The effect of overexpression CINAM on the inflorescence morphology of *C. lavandulifolium*

To verify the effect of CINAM on the inflorescence morphology of *C. lavandulifolium*, we constructed the transgenic lines of 35S::CINAM and made detailed observations of their phenotypic changes. Interestingly, the extent of changes in inflorescence morphology was not uniform throughout the plants. At the top of plants, WT lines plants produced 1–6 capitulum per compound corymbose synflorescence (Fig. 2A), whereas OE-CINAM lines produced 4–16 per compound corymbose synflorescence (Fig. 2B). The number of capitula in the OE-CINAM lines increased with the height of the branch (Fig. S2A, see online supplementary material), and the number of capitula on the bottom branches was lower than in the WT plants (Fig. S2B, see online supplementary material). This secondary branching pattern significantly altered the inflorescence morphology of *C. lavandulifolium*, resulting in the compound corymbose synflorescences also in the upper branches of the plant (Fig. S2A, see online supplementary material). Because boundary genes can also affect root growth [24, 27], we also observed root morphology in the OE-CINAM lines but did not observe any significant changes (Fig. S3, see online supplementary material).

Overexpression of CINAM also affected the morphology of the capitulum, with the OE-CINAM lines having a significantly smaller capitulum than the WT lines (Fig. 2C). The development of ray florets was significantly suppressed in the OE-CINAM lines, while the ray florets were still enveloped by the involucre in the first round of disc florets flowering. In addition, the state of ray florets development was not uniform (Fig. 2C). The corolla length of the disc florets showed the opposite trend, being longer in the OE-CINAM lines than the WT lines (Fig. 2E). The extent of variation in corolla length for both types of florets was also correlated with

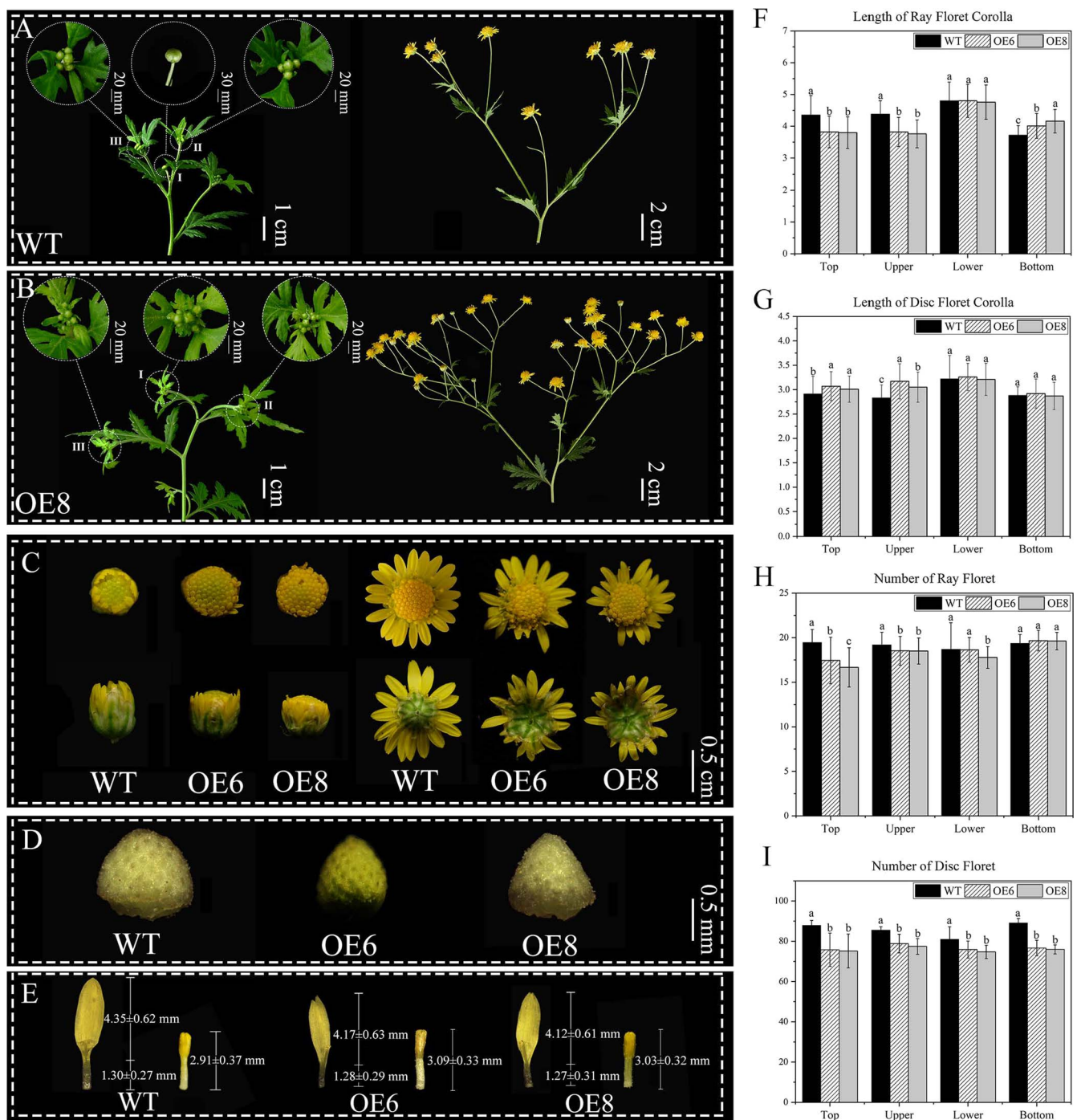


Figure 2. Effect of overexpression of *CINAM* on the morphology of *Chrysanthemum lavandulifolium* inflorescences. (A–B) Overexpression of *CINAM* caused a significant increase in the number of capitulum on top of plants. (C) Overexpression of *CINAM* resulted in developmental delayed ray floret corolla and elongated disc corolla. (D) Overexpression of *CINAM* caused changes in the receptacle morphology of the *C. lavandulifolium* and a decrease in the area of receptacle. (E) Overexpression of *CINAM* resulted in shortened ray floret corolla and elongated disc corolla. (F–G) Overexpression of *CINAM* caused a change in the length of both types of florets with the position. (H–I) Overexpression of *CINAM* caused a change in the number of both types of florets with the position height. Note: All phenotypic data were obtained from five independent plants. The lowercase letters represent the significance of differences between the three lines; where the letters are different, there is a significant difference ($P < 0.05$).

of *CINAM* significantly increased the expression of *cla-miR164* (Fig. 3D).

Possible *cla-miR164* target binding sites in *CINAM* were projected and ligated into pGreenII 0800-LUC containing 35S promoter and co-injected with pGreenII 62-SK with *cla-miR164* precursor sequence attached in the leaves of tobacco. The change in fluorescence value was then observed. The results showed that

cla-miR164 had a direct targeting and cleaving ability on *CINAM*. This targeting and cleaving ability was eliminated after 2-point mutations with synonymous substitutions in the targeting site of *CINAM* (Fig. 3E–G). To further determine the targeted degradation of *CINAM* by *cla-miR164* in *C. lavandulifolium*, the *Agrobacterium* GV3101 which contains blank and 35::*cla-miR164* pGreenII 62-SK plasmids was used and injected into *C. lavandulifolium* leaves

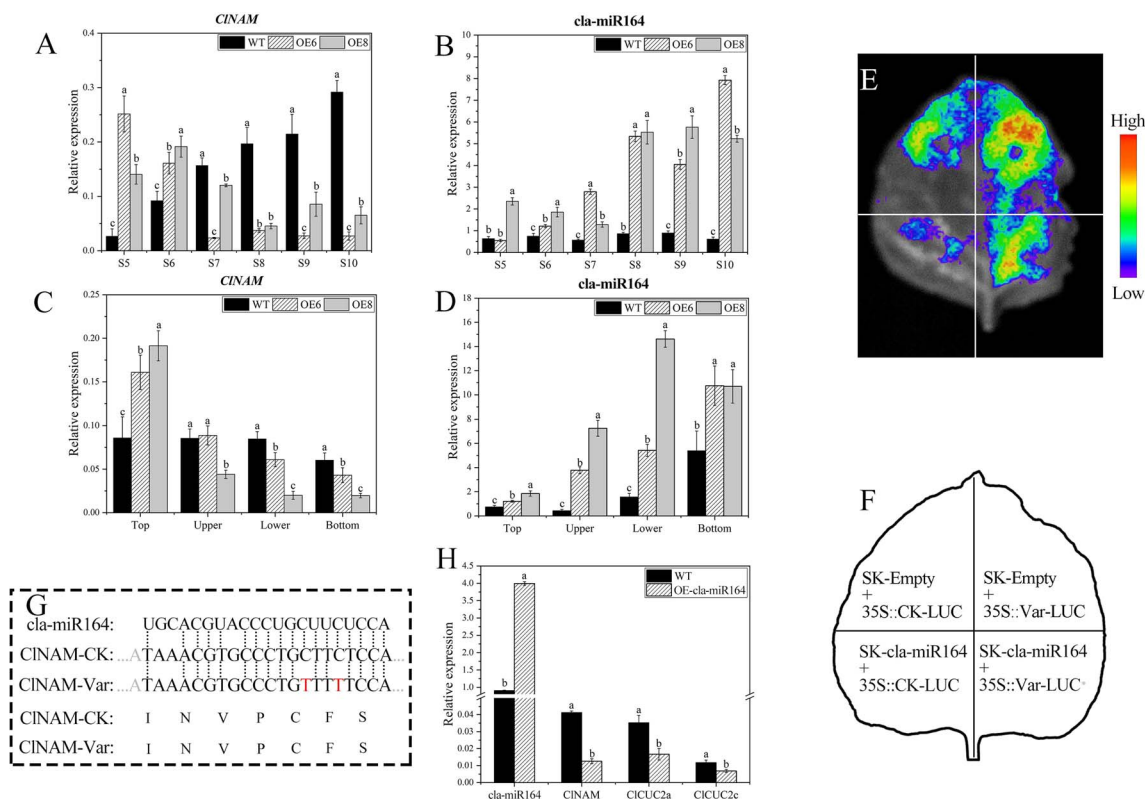


Figure 3. Involvement of *cla-miR164* in inflorescence architecture development through targeted cleavage of *CINAM* in *Chrysanthemum lavandulifolium*. (A–B) Expression changes of *CINAM* and *cla-miR164* during the capitulum developing from the top of *C. lavandulifolium*. (C–D) Expression changes of *CINAM* and *cla-miR164* in S6 reproductive buds of different heights in *C. lavandulifolium*. (E–F) Targeted cleavage ability of *cla-miR164* on *CINAM*. (G) The targeting sites of *CINAM* and sequences of *cla-miR164* in *C. lavandulifolium*, CK: Control Check, Var: Variant. (H) Expression changes of *cla-miR164*, *CINAM*, *CUC2a/c* in leaves of momentary overexpression *cla-miR164*. Note: The lowercase letters represent the significance of differences between lines; where the letters are different, there is a significant difference ($P < 0.05$).

and the expression of *cla-miR164* and downstream target genes was measured in the treated leaves (Fig. 3H). The results showed that the expression of *CINAM* was significantly reduced after overexpression of *cla-miR164* in the leaves of *C. lavandulifolium*. In previous reports, *CUC2* is a conserved target gene of *cla-miR164*, and we similarly observed that *CUC2a/c* expression was significantly downregulated in leaves of OE-*cla-miR164*.

The function of *cla-miR164* in *C. lavandulifolium* is to target and cleave the *CINAM*. The expression patterns of *CINAM* and *cla-miR164* during capitulum development and in reproductive shoots of different heights indicate that overexpression of *CINAM* leads to enriched *cla-miR164* levels and there are differences between top and bottom inflorescences. Eventually, this causes a specific pattern of phenotypic variation on the OE-*CINAM* lines. Therefore, we also determined that *CINAM* in OE-*CINAM* is not completely overexpressed, but presents a pattern of modified expression.

The transcriptional regulation of *CINAM* in relation to genes related to flower development

To investigate the molecular mechanism of *CINAM* regulation of inflorescence architectures in *C. lavandulifolium*, we selected reproductive buds at the S6 stage from the top of the plants, where *CINAM* expression was highest and phenotypic changes in inflorescence were most significant, for the construction of transcriptome libraries (Table S1, see online supplementary material). A total of 2566 differentially expressed genes were screened in the OE-*CINAM* lines, of which 556 genes were up-regulated and 2010 genes were down-regulated (Fig. S4, see online supplementary

material). Further screening of genes related to inflorescence development in the data set revealed that *CINAM*, *CUC2a*, and *CUC2c* were up-regulated among the boundary genes in the OE-*CINAM* lines. In addition, many ABCE-class genes of the MADS-box gene family, auxin response factors, and auxin transporter proteins were up-regulated in the OE-*CINAM* lines (Fig. S5, see online supplementary material).

In a previous study, we found that *CILBD18*, *CINAM*, *CUC2a*, and *CUC2c* show co-expression patterns during capitulum development and may have a direct upstream-downstream relationship [12]. We examined the expression of *CILBD18*, *CUC2a*, and *CUC2c* after the modification of *CINAM*. The results showed that *CUC2a* and *CUC2c* had a consistent expression pattern with *CINAM*, with the expression peak being advanced to the middle of floral primordium initiation stage (S6), while the expression at the corolla formation stage (S8–S10) was repressed, possibly by downstream genes directly regulated by *CINAM*. In contrast, *CILBD18* expression in the OE6 and OE8 lines varied widely and may not be a downstream gene regulated by *CINAM* (Fig. 4A). Analysis of the promoter sequences of *CUC2a* and *CUC2c* revealed the presence of *CINAM* binding sites on both of their promoter sequences (Fig. S6A, see online supplementary material). The results of Y1H experiments also indicated that *CINAM* was able to bind to these regions (Fig. 4B). A dual-luciferase assay revealed the highly significant transcriptional activation ability of *CINAM* for *CUC2a* and *CUC2c* (Fig. 4B).

Further analysis revealed there were two MADS-box genes and a conserved binding site for *LBD18* in the promoter sequence of

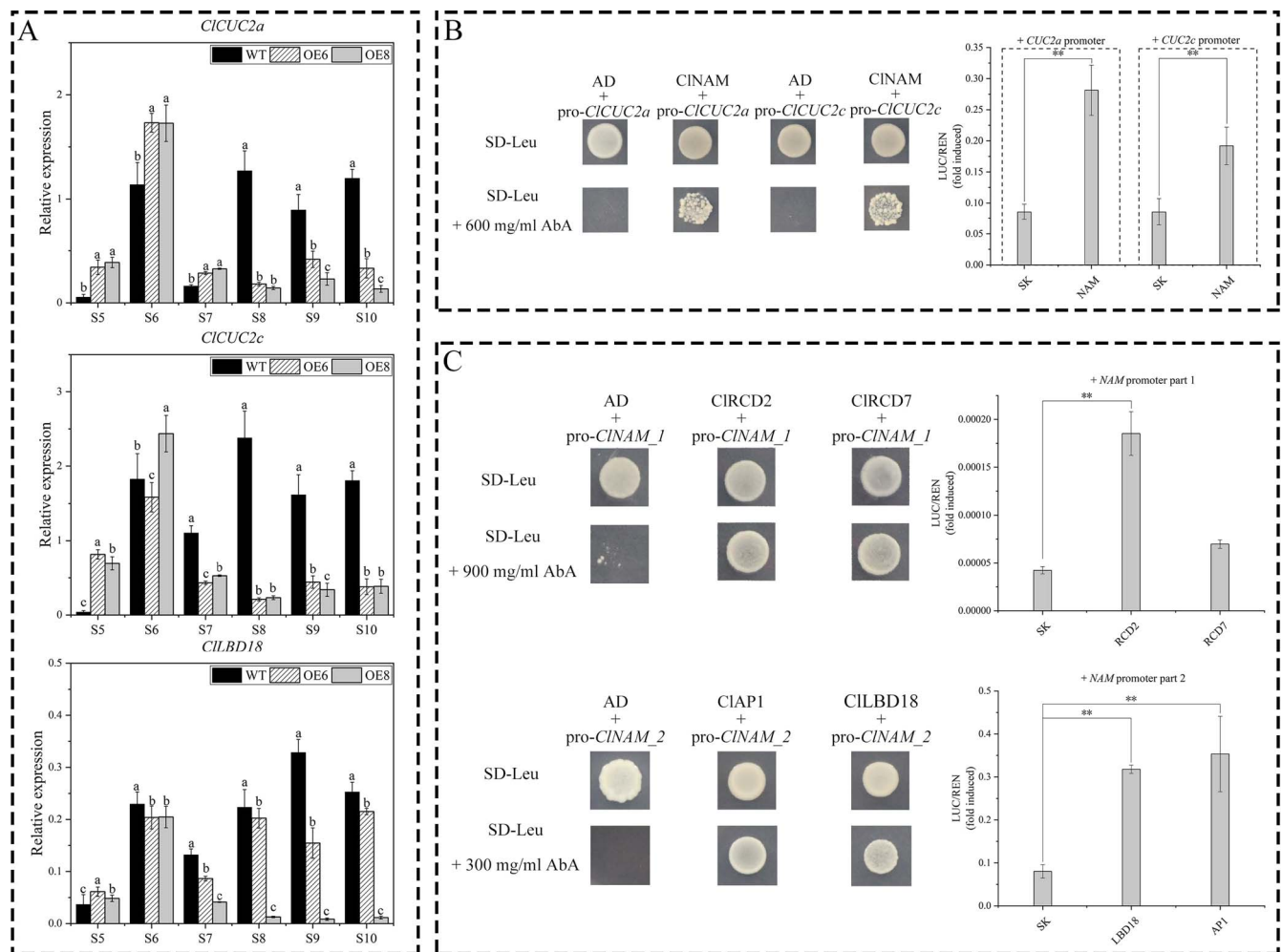


Figure 4. Up- and down-stream transcription factor screening of *CINAM*. (A) Expression changes of boundary genes *CILBD18*, *ClCUC2a*, and *ClCUC2c* in the OE-*CINAM* lines. (B) *CINAM* has transcriptional activation ability for *ClCUC2a* and *ClCUC2c*. (C) The expression of *CINAM* is significantly activated by *CILBD18*, the A-class gene *CIAP1*, and the E-class gene *CIRCD2*. Note: ** $P < 0.01$. The lowercase letters represent the significance of differences between the three lines; where the letters are different, there is a significant difference ($P < 0.05$).

CINAM (Fig. S6A, see online supplementary material). Y1H experiments revealed that the E-class genes *CIRCD2* and *CIRCD7* were able to bind in part 1, and *CILBD18* and the A-class gene *CIAP1* were able to bind in part 2 (Fig. 4C). The results of the dual luciferase assay showed that *CILBD18*, *CIAP1*, and *CIRCD2* all activated the expression of *CINAM* significantly.

These results suggest that the expression of *CINAM* is regulated by the MADS-box gene and the boundary gene *CILBD18*. Then, the *CINAM* activates the downstream *ClCUC2a* and *ClCUC2c*, forming a boundary gene regulatory network with *CINAM* as the central core. Combined with the phenotypic changes in the OE-*CINAM* lines, we suggest that this gene regulatory network is involved in the initiation of floret and flower primordia on the capitulum and compound corymbose synflorescence of *C. lavandulifolium*, regulating the number of florets per capitulum and capitulum of compound corymbose, which in turn affects the construction inflorescence morphology of *C. lavandulifolium*.

CINAM indirectly regulates the expression of ABCE-class genes

Up-regulated expression of many MADS-box genes was observed in the transcriptome data of the OE-*CINAM* lines. These genes are highly correlated with corolla development [25] and may

be responsible for the variation in corolla length of florets in the OE-*CINAM* lines. In a previous study, eight MADS-box genes differentially expressed in the corollas of ray and disc florets of *C. lavandulifolium* were identified, among which the B-class gene *CIAP3* and *CIPIa*, the E-class gene *CIRCD1/3/4/7* were highly expressed in the ray florets. The A-class gene *CIAP1* and the C-class gene *CIAG1* were highly expressed in the corollas of disc florets [26].

The expression of *CINAM* and the above-mentioned MADS-box genes were examined in the corollas of WT and OE-*CINAM* lines. The expression of *CINAM* was significantly increased in ray floret corollas and significantly decreased in disc floret corollas in the OE-*CINAM* lines (Fig. 5A). In addition, the expression of *CIRCD4* and *CIRCD7* were up-regulated, and the expression of *CIAP3*, *CIPIa*, *CIAP1*, and *CIAG1* were down-regulated in the ray floret corollas of OE-*CINAM* lines. The overall gene expression pattern was close to that of the disc floret corollas in the WT lines (Fig. 5B). These results suggest that *CINAM* may be a key gene in maintaining the morphological development of disc corollas. When *CINAM* was ectopically expressed in ray corollas, the ray corollas were shortened, and development was delayed, and the expression patterns of the associated MADS-box were all similar to those of disc corollas of the WT lines.

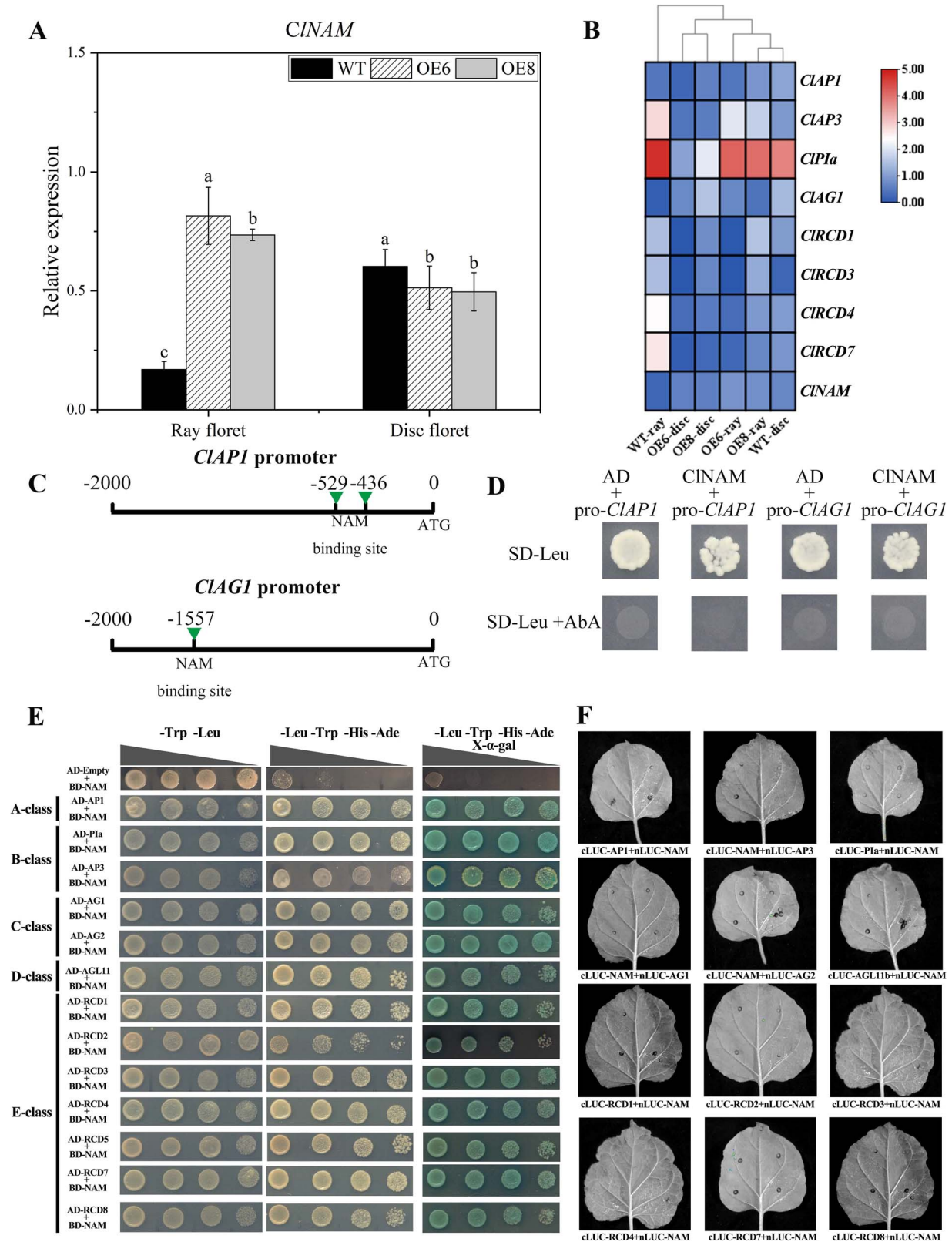


Figure 5. Modified *CINAM* affects the expression of MADS-box genes that control corolla development in two types of florets. **(A)** Expression of *CINAM* in the corollas of both types of florets after modified of *CINAM*. **(B)** Changes in expression of key MADS-box genes in the corollas of both types of florets after modified of *CINAM*. **(C–D)** *CINAM* fails to bind to *CIAP1* and *CLAG1* promoter elements. **(E–F)** *CINAM* was detected to widely interact with ABC(D)E-class protein in *Chrysanthemum lavandulifolium* in Y2H system, but no positive results were observed in the luciferase complementation assay. Note: The lowercase letters represent the significance of differences between the three lines; where the letters are different, there is a significant difference ($P < 0.05$).

By analysing the promoter sequences of *CIRCD1*, *CIRCD4*, *ClAP3*, *ClPla*, *ClAP1*, and *ClAG1*, we found possible binding sites of *CINAM* in the promoter sequences of *ClAP1* and *ClAG1*. However, the results of the Y1H assay showed that *CINAM* did not bind to these sites (Fig. 5C and D). This suggests that *CINAM* does not directly regulate the expression of these MADS-box genes. There may be some unknown transcription factors between the *CINAM* and MADS-box genes. In addition, we found that *CINAM* widely interacts with ABC(D)E-class protein in *C. lavandulifolium* by Y2H assay (Fig. 5E), but no corresponding positive result resulted from further luciferase complementation assay (LCA) and bimolecular fluorescence complementation (BiFC) (Fig. 5F; Fig. S7, see online supplementary material).

These results suggest that the change in corolla length of florets in the OE-*CINAM* lines result from the ectopic expression of *CINAM* followed by altered expression of related ABC(D)E-class genes. Although they are correlated in expression patterns, there is no evidence of a direct transcriptional regulatory relationship between *CINAM* and these ABC(D)E-class genes. Their protein-level interactions can only be detected in the Y2H system, with the possibility of false positives.

Discussion

Predicted targets of miR164 include mRNAs encoding five members of the NAC domain transcription factor family in Arabidopsis [27]. Of these, *NAC1* is involved in the transduction of auxin signals for lateral root development, and *CUC1/CUC2* are involved in meristem development and aerial organ separation, whereas the functions of *At5g07680* and *At5g61430* have not yet been defined [28]. In this study, we found the potential function of *CINAM*, which is the orthologous gene of *At5g07680* and *At5g61430*. Further study presents a boundary gene regulatory network with *cla-miR164-CINAM* as the core. The results showed that *CINAM* was activated by the *ClAP1* and *CIRCD2* as well as the boundary gene *ClLBD18*. Activating the expression of *ClCUC2a/c*, which induced the initiation of floret and inflorescence primordia on the inflorescence meristem, regulated the differentiation of the two types of florets and the capitula in *C. lavandulifolium*. This network influenced the establishment of primary and secondary inflorescence morphology in *C. lavandulifolium* in terms of the number of flowers (Fig. 6). This finding provides new insights into the early inflorescence development process of chrysanthemums and suggests a new pathway in the molecular regulatory network of regulation of chrysanthemums inflorescence architecture.

cla-miR164-CINAM module regulates the initiation of *C. lavandulifolium* floret and flower primordia

In previous studies of Arabidopsis, boundary genes such as *LBD18* and *CUCs* through the regulation auxin concentration and *KNOX* expression to inhibit the cell division, but there is no direct regulative relationship between them [14]. In the present study, we found that *CINAM* is located between *ClLBD18* and *ClCUC2s* in the regulatory network and transmits transcriptional regulatory signals to the boundary genes. Because the capitulum structure is more elaborate in Asteraceae than in many other plants, we propose that this hierarchical transmission of regulatory signals from boundary genes is crucial for the maintenance of this complex inflorescence morphology.

Interestingly, the trends in the number of flowers in the capitulum (primary inflorescence) and in the compound corymbose synflorescence (secondary inflorescence) were different in the

OE-*CINAM* lines. The number of both types of florets in the capitulum was significantly reduced in the OE-*CINAM* lines, and the number of disc florets in the disc center was particularly reduced. In contrast, the number of capitula increased significantly in the compound corymbose synflorescence of the OE-*CINAM* lines. This contrast is mainly due to the different patterns of development in the two types of inflorescences. Capitula have a specific developmental pattern in which the highly compressed inflorescence axis (receptacle) is in dynamic equilibrium with the initiation of the floral primordium [10]. When the expression peak of *CINAM* is advanced in the OE-*CINAM* lines, the receptacle completes all florets before it is fully developed. As a result, the morphology of the receptacle is altered and the surface area is reduced, leading to a decrease in the number of florets. In the OE-*CINAM* lines, the disc florets in the center of the disc were more affected than the ray florets at the margins, indicating that *CINAM* regulates the initiation of disc flower primordia during receptacle development. In contrast, in the compound corymbose synflorescence of *C. lavandulifolium*, the capitulum developed gradually from the top to bottom when the inflorescence axis was fully developed, and *CINAM* directly promoted the initiation of the capitulum primordia.

This study also revealed the *CINAM* was targeted and cleaved by *cla-miR164* in *C. lavandulifolium*. The *cla-miR164* was up-regulated when in ectopic expression and overexpression of *CINAM* and removes excess *CINAM* to maintain normal inflorescence morphology. This mechanism led to inconsistent results in the extent of inflorescence morphological variation of the OE-*CINAM* lines. In *Zea mays*, *Oryza sativa*, *Arabidopsis thaliana*, and *M. truncatula*, miRNA164 exhibited targeted cleavage effects on NAC gene family members to maintain normal organ morphology and function, suggesting that such regulatory effects are conserved across species [19–21, 24]. It has been shown that miRNA164 acts in conjunction with *NAM/CUC* as a homeostatic mechanism to regulate auxin signaling [27, 29, 30], while the localized enrichment of auxin is essential for floret patterning in Asteraceae [31]. In addition, auxin also has a regulatory role in the corolla morphology of ray floret in chrysanthemums [32, 33]. In the present study, many differential expressions of auxin transporter proteins and auxin response factors were found in the OE-*CINAM* lines, suggesting that *cla-miR164-CINAM* may affect inflorescence architectures in chrysanthemums by regulating auxin signaling (Fig. S5, see online supplementary material).

In conclusion, our results suggest that the *cla-miR164-CINAM* module facilitates the initiation of floral and inflorescence primordium, and maintains a dynamic balance between the development of inflorescence meristem and the initiation of floral primordium in the capitulum. This function both affected the architectures of capitulum and the compound corymbose synflorescence (Fig. 6).

CINAM has a complex regulatory relationship with ABC(D)E class genes

AP1 is not only the A-class gene that specifies sepal and petal identity but also an important floral meristem (FM) maintenance gene, regulated by the upstream *LEAFY (LFY)* gene activating floral meristem initiation [34–37]. *SEPALATA (SEP)* in Arabidopsis is highly redundant in its function to determine floral organ identity, but *RCD*, the ortholog of the *SEP* in plants of the Asteraceae family, undergoes significant expansion and functional divergence. *RCD2/3/4/7* are not only involved in organizing the inflorescence meristem at the capitulum, but also in the orderly differentiation of the inflorescence meristem (IM) and floral meristem at the

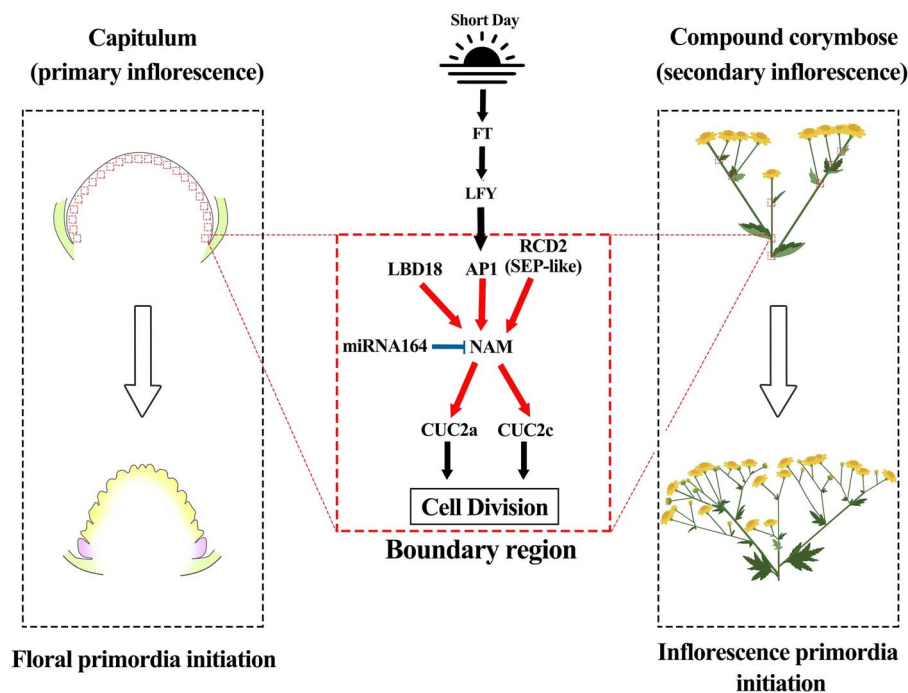


Figure 6. The boundary gene regulatory network with *cl-miR164-CINAM* as the core is involved in the inflorescence architectures of *Chrysanthemum lavandulifolium*. Note: The black arrows indicate the previous findings, while the red arrows indicate the original results in this study. The blue line segment indicates the targeted degradation effect of *cl-miR164* on *CINAM*. The red boxes indicate the boundary region on the inflorescence meristem.

capitulum [38]. In this study, we found that *CINAM* is directly activated by *CLAP1* and *CIRCD2*, suggesting that the boundary genes are located downstream of the floral induction network and initiate the floral meristem after receiving upstream floral induction signals.

In situ hybridization showed that *CINAM* was expressed predominantly in disc florets during the corolla formation stage. qRT-PCR results also indicated that *CINAM* was expressed significantly more in disc corollas than in ray corollas, suggesting that *CINAM* may also have a function in maintaining morphological differences between the corollas of the two types of florets (Fig. 5A). Although many ABC(D)E-class genes were found to be differentially expressed in the transcriptome data and in qRT-PCR experiments in the OE-*CINAM* lines, which were accompanied by significant changes in corolla length, no evidence was found for a direct association of *CINAM* with these ABC(D)E-class genes. Although *CINAM* showed wide protein interactions with ABC(D)E-class genes in the Y2H assay, no corresponding positive results were observed in the luciferase complementation assay. A similar decrease in expression of all ABC(D)E-class genes with *MtNAM* was observed in the *nam* mutant from *M. truncatula*, but the regulatory relationship between the two was not elucidated [16]. These results suggest that there is a close relationship between *NAM* and these floral organ identity-determining genes, but no evidence has shown any directly targeted and regulated during floral organs development. We hypothesize that there are still unknown hub genes between *CINAM* and ABC(D)E-class genes, or that *CINAM* affects floral organ development through other regulatory pathways that are not causally related to changes in the expression of ABC(D)E-class genes.

Materials and methods

Plant materials and genetic transformation

The G1 line of *C. lavandulifolium* used in the present study was the same as *C. lavandulifolium* genome sequencing [12]. The full-

length CDS (coding sequence) of *CINAM* was cloned into the binary vector pBI121 and used to transform *Agrobacterium* GV3101. The transgenic *C. lavandulifolium* plants were obtained by the leaf disc transformation. The MS medium containing 0.1 mg 6-BA + 2.0 mg/L NAA + 400 mg/L Carb was used for inducing the transformation. The MS medium containing 7 mg/L Kan + 400 mg/L Carb was used for selection. Positive plants were detected by PCR using primers 35S (F: 5'-GACGCACAATCCCACATATCC-3') and NOS (R: 5'-AATCATCGCAAGACCGGC-3').

Growth conditions and phenotypic observations

These materials were planted with peat: vermiculite = 1:1. The temperature was $22 \pm 1^\circ\text{C}$ and the light intensity was 4000 lx. The nutritive growth was carried out under long daylight (16 h light/8 h dark). After they grew 14 leaves, they were transferred to short daylight (12 h light/12 h dark) for reproductive growth. Phenotypic observations and statistics were made at flowering. Five biological replicates were used to confirm the reliability of the observations.

Phylogenetic analysis

The NAC protein sequences of Arabidopsis, which are used as a reference sequence for BLAST were downloaded from the Plant Transcription Factor Database (<http://plantfdb.gao-lab>) [39]. Genomic data of *C. lavandulifolium* (PRJNA681093) [12] and *Mikania micrantha* (PRJNA528368) [40] were downloaded from NCBI (<https://www.ncbi.nlm.nih.gov/>). *Helianthus annuus* (PRJNA345532) [41], *Lactuca sativa* (PRJNA173551) [42] were downloaded from EnsemblPlants (<http://plants.ensembl.org/index.html>). *C. nankingense* [43] was downloaded from the Chrysanthemum Genome Database (<http://www.amwayabc.com/zh-cn/index.html>). *C. makinoi* [44] was downloaded from <https://www.chrysanthemumgenome.wur.nl/>. *C. x morifolium* (PRJNA796762) [33] was downloaded from the Figshare (<https://doi.org/10.6084/m9.figshare.21655364.v2>) and *C. seticuspe* (Gojo-0

v1) [45] was downloaded from the Plant Garden database (<https://plantgarden.jp/en/list/t1111766/genome/t1111766.G002>).

NAM/CUC members in six Asteraceae plants were identified in TBtools v1.098765 by BLAST (E-value cut-off of $1e^{-5}$) [46]. The AtNAC sequences were used as reference sequences. Sequence alignment of the obtained sequences was performed using MUSCLE [47]. The trimAI (-automated1 option) [48] was used to trim poorly aligned sequences and reserve reliable comparison results. The best-fit model (JTT+I+G4) was selected according to the BIC and the maximum likelihood (ML) phylogenetic tree was constructed in IQtree v2 (bootstrap replicates = 1000) [49]. The final phylogenetic tree was embellished in iTOL (<https://itol.embl.de/>).

Subcellular localization

The CDS of CINAM, which has had the termination codon removed was cloned into the binary vector pBI121-GFP. The recombinant vectors were transformed into *Agrobacterium* GV3101 and injected into *Nicotiana benthamiana* leaves. The treated tobacco was incubated for 48 h (24 h dark/24 h light) and the subcellular localization of fluorescent proteins was observed under a laser confocal microscope (SP8-WLL, Leica Microsystems, Wetzlar, Germany).

In situ hybridization

The floral organs were collected from different developmental stages as previously described [10]. The desired target fragment is amplified in genomic DNA using CINAM gene-specific primers (F: 5'-GGGTTTCGGTTTCATCCAAG-3' and R: 5'-GGTAGGATACTTCTTATCCCTCACA-3', 198 bp). After sequencing to obtain the reverse inserted plasmid, probes were constructed using the Roche DIG RNA Labeling Kit (SP6/T7). Detection time was 16 h.

RNA extraction and qRT-PCR analysis

All samples were sampled as previously described [10]. The morphology of the sampled material is shown in Fig. S8 (see online supplementary material). The total RNA was extracted from the collected plant materials using the Plant RNA Rapid Extraction Kit (HUAYUEYANG Biotechnology, Beijing, China) and treated with RNase-free DNaseI to digest DNA. The first-strand cDNA was synthesized using Transcriptor First Strand cDNA Synthesis Kit (TaKaRa, Dalian, China) and miRNA 1st Strand cDNA Synthesis Kit (by tailing A) (Novozymes, Nanjing, China) with 1 μ g of total RNA.

Gene and cla-miR164 expression analysis was performed by real-time quantitative reverse transcription-PCR (qRT-PCR), which was performed using a qTOWER3 (Analytik Jena AG, Germany), SYBR Premix Ex Taq (Takara Bio Inc., Shiga, Japan) and miRNA Universal SYBR gPCR Master Mix (Novozymes, Nanjing, China) were used for qRT-PCR in gene and cla-miR164, respectively. Three biological replicates were used to confirm the reliability of the results. ClSAND and ClU6 were used as an internal control gene for qRT-PCR. The primers for qRT-PCR are shown in Table S2 (see online supplementary material). The $2^{-\Delta\Delta Ct}$ method was used to analyse qRT-PCR data.

Transcriptome sequencing

These materials were taken from the S6 reproductive buds of the top of the wild-type and OE-CINAM lines of *C. lavandulifolium*. A total of six libraries (WT-1, WT-2, WT-3, OE8-1, OE8-2, OE8-3) were constructed for RNA-seq. In conclusion, total RNA was extracted from the samples and the cDNA libraries were sequenced on the

Illumina NovaSeq 6000 sequencing platform (Illumina, San Diego, CA, USA). Sequencing was performed by Biomarker Technologies (Beijing, China). The data were processed as previously described [12].

Transcriptional activation assay

The coding regions of CINAM, CILBD18, CIAP1, and CIRCD2/7 were cloned into the pGADT7 (AD) vector. The promoters of CINAM, CUC2a/c, CIAP1, and CIAG1 were isolated from *C. lavandulifolium* gDNA and cloned into the pAbAi vector. The Yeast single hybridization (Y1H) assay used the Matchmaker™ Gold Yeast Two-Hybrid System (Clontech, Mountain View, CA, USA). The yeast strain is Y1H Gold. The blank pGADT7(AD) vector was used as a negative control for this assay.

The coding regions of CINAM, CILBD18, CIAP1, and CIRCD2/7 were cloned into pGreenII 62-SK. The promoters of CINAM, CUC2a/c, CIAP1, and CIAG1 were cloned into pGreenII 0800-LUC. The blank pGreenII 62-SK vector was used as a negative control for this assay. The recombinant vectors were transformed into *Agrobacterium* GV3101 and injected into *N. benthamiana* leaves. The treated tobacco was incubated for 48 h (24 h dark/24 h light). The Dual-Luciferase Reporter Assay System (Promega, Madison, WI, USA) and the multifunctional enzyme labeler EnVision (PerkinElmer, USA) were used for sample extraction and signal detection. Dual luciferase imaging was accomplished using the molecular imaging system LB983 NightOwl II (Berthold Technologies, Bad Wildbad, Germany).

Protein interaction assay

The coding sequences of all genes to be tested were cloned into the pGADT7 (AD) and pGBKT7 (BD) vectors, respectively, for Yeast two hybrid (Y2H) assay. The experimental procedure was performed as previously described [26].

The coding sequences of all genes to be tested were cloned into pCAMBIA1300-cLUC and pCAMBIA1300-nLUC vectors, respectively (requiring the removal of the termination codon if they cloned into pCAMBIA1300-nLUC), and luciferase complementation assay was performed. The experimental procedure was as previously described [26]. Using the same method, the gene to be tested was cloned into the pSPYCE and pSPYNE173. The positive control plasmids and experimental procedure of BiFC were in reference to Lu et al. [50].

Cl-miR164-guided cleavage assay

The precursor sequence of cla-miR164 was isolated using *C. lavandulifolium* genomic information [12] and cloned into pGreenII 62-SK. The 35S promoter fragment from the pBI121 vector was ligated to pGreenII 0800-LUC, designated GreenII 0800-35S::LUC. The cla-miR164 targeting site sequence in CINAM was cloned into GreenII 0800-35S::LUC. In addition, the sequence was point mutated at two sites and also cloned into GreenII 0800-35S::LUC. The recombinant vectors were transformed into *Agrobacterium* GV3101 and injected into *N. benthamiana* leaves. The treated tobacco was incubated for 48 h (24 h dark/24 h light) and detected using the molecular imaging system LB983 NightOwl II (Berthold Technologies, Bad Wildbad, Germany).

Statistical analysis

All data were analysed using IBM SPSS Statistics 23.0 (SPSS Inc.; Chicago, IL, USA) for one-way analysis of variance followed by Duncan's test. The values are represented as the means \pm SD. $P < 0.05$ was considered as statistically significant.

Acknowledgments

This work was supported by National Natural Science Foundation of China (No.32371948, No. 31530064, and No. 31471907).

Author contributions

S.D, J.L, and X.W. conceived the study. J.L and X.W completed the main work. Q.Z. and Y.P. analysed the data. Y.T., J.W., B.L., and Y.D. contributed to planting material and phenotype data observation. J.L. completed the first draft. S.D. and X.W. revised the manuscript. All authors read and approved the final manuscript.

Date availability

Raw sequence data were submitted to the Sequence Read Archive (SRA) database of the National Center for Biotechnology Information (NCBI) (accession number: [PRJNA956717](https://www.ncbi.nlm.nih.gov/PRJNA956717)).

Conflict of interest statement:

The authors declare no competing interests.

Supplementary data

Supplementary data is available at *Horticulture Research* online.

References

- Broholm SK, Pöllänen E, Ruokolainen S. et al. Functional characterization of B class MADS-box transcription factors in *Gerbera hybrida*. *J Exp Bot*. 2010;**61**:75–85
- Elomaa P, Zhao Y, Zhang T. Flower heads in Asteraceae—recruitment of conserved developmental regulators to control the flower-like inflorescence architecture. *Hort Res*. 2018;**5**:36
- Sasaki K, Yoshioka S, Aida R. et al. Production of petaloid phenotype in the reproductive organs of compound flowerheads by the co-suppression of class-C genes in hexaploid *Chrysanthemum morifolium*. *Planta*. 2021;**253**:1–16
- Broholm SK, Tähtiharju S, Laitinen RA. et al. A TCP domain transcription factor controls flower type specification along the radial axis of the *Gerbera* (Asteraceae) inflorescence. *PNAS*. 2008;**105**:9117–22
- Tähtiharju S, Rijpkema AS, Vetterli A. et al. Evolution and diversification of the CYC/TB1 gene family in Asteraceae—a comparative study in gerbera (Mutisieae) and sunflower (Heliantheae). *Mol Biol Evol*. 2012;**29**:1155–66
- Juntheikki-Palovaara I, Tähtiharju S, Lan T. et al. Functional diversification of duplicated CYC2 clade genes in regulation of inflorescence development in *Gerbera hybrida* (Asteraceae). *Plant J*. 2014;**79**:783–96
- Wen X, Qi S, Huang H. et al. The expression and interactions of ABCE-class and CYC2-like genes in the capitulum development of *Chrysanthemum lavandulifolium* and *C. × morifolium*. *Plant Growth Regul*. 2019;**88**:205–14
- Huang D, Li X, Sun M. et al. Identification and characterization of CYC-like genes in regulation of ray floret development in *Chrysanthemum morifolium*. *Front Plant Sci*. 2016;**7**:1633
- Zhang CJ, Rong YL, Jiang CK. et al. Co-option of a carotenoid cleavage dioxygenase gene (*CCD4a*) into the floral symmetry gene regulatory network contributes to the polymorphic floral shape–color combinations in *Chrysanthemum sensu lato*. *New Phytol*. 2022;**236**:1197–211
- Wen X, Qi S, Yang L. et al. Expression pattern of candidate genes in early capitulum morphogenesis of *Chrysanthemum lavandulifolium*. *Sci Hortic*. 2019;**252**:332–41
- Pu Y, Huang H, Wen X. et al. Comprehensive transcriptomic analysis provides new insights into the mechanism of ray floret morphogenesis in chrysanthemum. *Genomics*. 2020;**21**:1–16
- Wen X, Li J, Wang L. et al. The *Chrysanthemum lavandulifolium* genome and the molecular mechanism underlying diverse capitulum types. *Hort Res*. 2022;**9**:uhab022
- Souer E, van Houwelingen A, Kloos D. et al. The no apical meristem gene of petunia is required for pattern formation in embryos and flowers and is expressed at meristem and primordia boundaries. *Cell*. 1996;**85**:159–70
- Žádníková P, Simon R. How boundaries control plant development. *Curr Opin Plant Biol*. 2014;**17**:116–25
- Shuai B, Reynaga-Pena CG, Springer PS. The lateral organ boundaries gene defines a novel, plant-specific gene family. *Plant Physiol*. 2002;**129**:747–61
- Cheng X, Peng J, Ma J. et al. NO APICAL MERISTEM (MtNAM) regulates floral organ identity and lateral organ separation in *Medicago truncatula*. *New Phytol*. 2012;**195**:71–84
- Jiao K, Li X, Guo Y. et al. Regulation of compound leaf development in mungbean (*Vigna radiata* L.) by CUP-SHAPED COTYLEDON/NO APICAL MERISTEM (CUC/NAM) gene. *Planta*. 2019;**249**:765–74
- Hendelman A, Stav R, Zemach H. et al. The tomato NAC transcription factor SINAM2 is involved in flower-boundary morphogenesis. *J Exp Bot*. 2013;**64**:5497–507
- Shan T, Fu R, Xie Y. et al. Regulatory mechanism of maize (*Zea mays* L.) miR164 in salt stress response. *Russ J Genet*. 2020;**56**:835–42
- Chang Z, Xu R, Xun Q. et al. OsmiR164-targeted OsNAM, a boundary gene, plays important roles in rice leaf and panicle development. *Plant J*. 2021;**106**:41–55
- Wang J, Bao J, Zhou B. et al. The Osa-miR164 target OsCUC1 functions redundantly with OsCUC3 in controlling rice meristem/organ boundary specification. *New Phytol*. 2021;**229**:1566–81
- Weir I, Lu J, Cook H. et al. CUPULIFORMIS establishes lateral organ boundaries in *antirrhinum*. *Development*. 2004;**131**:915–22
- Aida M, Tasaka M. Genetic control of shoot organ boundaries. *Curr Opin Plant Biol*. 2006;**9**:72–7
- Li J, Guo G, Guo W. et al. miRNA164-directed cleavage of ZmNAC1 confers lateral root development in maize (*Zea mays* L.). *BMC Plant Biol*. 2012;**24**:1–14
- Theißen G, Melzer R, Rümpler F. MADS-domain transcription factors and the floral quartet model of flower development: linking plant development and evolution. *Development*. 2016;**143**:3259–71
- Li J, Zhang Q, Kong D. et al. Genome-wide identification of the MIKCC-type MADS-box gene family in *Chrysanthemum lavandulifolium* reveals their roles in the capitulum development. *Front Plant Sci*. 2023;**14**:1100
- Guo HS, Xie Q, Fei JF. et al. MicroRNA directs mRNA cleavage of the transcription factor NAC1 to downregulate auxin signals for Arabidopsis lateral root development. *Plant Cell*. 2005;**17**:1376–86
- Mallory AC, Dugas DV, Bartel DP. et al. MicroRNA regulation of NAC-domain targets is required for proper formation and separation of adjacent embryonic, vegetative, and floral organs. *Curr Biol*. 2004;**14**:1035–46
- Shi M, Hu X, Wei Y. et al. Genome-wide profiling of small RNAs and degradome revealed conserved regulations of miRNAs on auxin-responsive genes during fruit enlargement in peaches. *Int J Mol Sci*. 2017;**18**:2599

30. Nikovics K, Blein T, Peaucelle A. et al. The balance between the *MIR164A* and *CUC2* genes controls leaf margin serration in *Arabidopsis*. *Plant Cell*. 2006;**18**:2929–45
31. Zhang T, Cieslak M, Owens A. et al. Phyllotactic patterning of gerbera flower heads. *PNAS*. 2021;**118**:e2016304118
32. Pu Y, Liao M, Li J. et al. Floral development stage-specific transcriptomic analysis reveals the formation mechanism of different shapes of ray florets in chrysanthemum. *Genes*. 2023;**14**:766
33. Song A, Su J, Wang H. et al. Analyses of a chromosome-scale genome assembly reveal the origin and evolution of cultivated chrysanthemum. *Nat Commun*. 2023;**14**:2021
34. Litt A. An evaluation of A-function: evidence from the *APETALA1* and *APETALA2* gene lineages. *Int J Plant Sci*. 2007;**168**:73–91
35. Han Y, Zhang C, Yang H. et al. Cytokinin pathway mediates *APETALA1* function in the establishment of determinate floral meristems in *Arabidopsis*. *PNAS*. 2014;**111**:6840–5
36. Blümel M, Dally N, Jung C. Flowering time regulation in crops—what did we learn from *Arabidopsis*? *Curr Opin Biotechnol*. 2015;**32**:121–9
37. Rhoades MW, Reinhart BJ, Lim LP. et al. Prediction of plant microRNA targets. *Cell*. 2002;**110**:513–20
38. Zhang T, Zhao Y, Juntheikki I. et al. Dissecting functions of *SEPALLATA*-like MADS box genes in patterning of the pseudanthial inflorescence of *Gerbera hybrida*. *New Phytol*. 2017;**216**:939–54
39. Tian F, Yang DC, Meng YQ. et al. PlantRegMap: charting functional regulatory maps in plants. *Nucleic Acids Res*. 2020;**48**:D1104–13
40. Liu BO, Yan J, Li W. et al. *Mikania micrantha* genome provides insights into the molecular mechanism of rapid growth. *Nat Commun*. 2020;**11**:340
41. Badouin H, Gouzy J, Grassa CJ. et al. The sunflower genome provides insights into oil metabolism, flowering and Asterid evolution. *Nature*. 2017;**546**:148–52
42. Reyes-Chin-Wo S, Wang Z, Yang X. et al. Genome assembly with in vitro proximity ligation data and whole-genome triplication in lettuce. *Nat Commun*. 2017;**8**:14953
43. Song C, Liu Y, Song A. et al. The *Chrysanthemum nankingense* genome provides insights into the evolution and diversification of chrysanthemum flowers and medicinal traits. *Mol Plant*. 2018;**11**:1482–91
44. van Lieshout N, van Kaauwen M, Kodde L. et al. De novo whole-genome assembly of *Chrysanthemum makinoi*, a key wild chrysanthemum. *G3 (Bethesda)*. 2022;**12**:jkab358
45. Nakano M, Hirakawa H, Fukai E. et al. A chromosome-level genome sequence of *Chrysanthemum seticuspe*, a model species for hexaploid cultivated chrysanthemum. *Commun Biol*. 2021;**4**:1167
46. Chen C, Chen H, Zhang Y. et al. TBtools: an integrative toolkit developed for interactive analyses of big biological data. *Mol Plant*. 2020;**13**:1194–202
47. Edgar RC. MUSCLE: multiple sequence alignment with high accuracy and high throughput. *Nucleic Acids Res*. 2004;**32**:1792–7
48. Capella-Gutiérrez S, Silla-Martínez JM, Gabaldón T. trimAl: a tool for automated alignment trimming in large-scale phylogenetic analyses. *Bioinformatics*. 2009;**25**:1972–3
49. Minh BQ, Schmidt HA, Chernomor O. et al. IQ-TREE 2: new models and efficient methods for phylogenetic inference in the genomic era. *Mol Biol Evol*. 2020;**37**:1530–4
50. Lu C, Qu J, Deng C. et al. The transcription factor complex CmAP3-CmPI-CmUIF1 modulates carotenoid metabolism by directly regulating carotenogenic gene *CmCCD4a-2* in chrysanthemum. *Hort Res*. 2022;**9**:uhac020